Food Chemistry 484 (2025) 144494

Contents lists available at ScienceDirect

Food Chemistry

journal homepage: www.elsevier.com/locate/foodchem

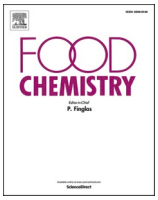

Tetrabutylammonium hydroxide and zinc salts in cellulose-based colloidal systems enhance fruit shelf life

Andrea Brattelli [a], Maria Chiara Sportelli [a,b], Rosaria Anna Picca [a,b], Nicola Cioffi [a,b], Mara Pasqualicchio [c], Ornella Incerti [c], Simona Marianna Sanzani [c], Luigi Gentile [a,b,*]

[a] Department of Chemistry, University of Bari Aldo Moro, Via Orabona 4, 70126, Bari, Italy
[b] Centre for Colloid and Surface Science (CSGI), Bari Unit, Via della Lastruccia 3, 50019 Sesto Fiorentino, Italy
[c] Dipartimento di Scienze del Suolo, della Pianta e degli Alimenti, University of Bari Aldo Moro, Via Amendola 165/A, 70126 Bari, Italy

ARTICLE INFO

Keywords:
Polysaccharides
Antifungal
Tetrabutylammonium hydroxide
Zinc salts
Shelf life
Food pads
Active colloids

ABSTRACT

This study explores the development of cellulose-based active colloidal systems to enhance the antimicrobial properties of absorbent food pads and prolong the shelf life of cherry tomatoes. Food pads impregnated with colloidal systems made of microcrystalline cellulose dissolved in tetrabutylammonium hydroxide (TBAH) with zinc salts ($ZnCl_2$ and $ZnSO_4$) were tested for their antifungal efficacy. *In vitro* results revealed complete fungal suppression by TBAH alone and in combination with $ZnCl_2$. The interaction between TBAH and $ZnSO_4$ exhibited synergistic antifungal activity, while an additive effect was observed with $ZnCl_2$. *In vivo* tests showed a significant reduction in fruit rot, with $ZnCl_2$-treated pads reducing rot by 91 % after 14 days. TBAH was partially bound to cellulose chains, minimizing the risk of fruit contamination, as confirmed by ^1H nuclear magnetic resonance.

1. Introduction

Food pads are absorbent materials used in food packaging to remove excess liquids and regulate moisture, helping in preserving the freshness and quality of perishable foods such as meat, poultry, fish, and small fruits. Active packaging is a system in which the packaging is modified to maintain or improve the sensory, safety and quality aspects of the food. (Ahmed et al., 2022; Kadirvel et al., 2025; Kumari et al., 2024; Su et al., 2025) Antimicrobial food packaging is one of the main novelties in the field of food packaging. (He et al., 2024;Stroescu et al., 2019; Xu et al., 2024) Inorganic salts, essential oils and polysaccharides have been investigated as antimicrobial active substances. (Stroescu et al., 2019; Xu et al., 2024).

Carbohydrates such as cellulose, being renewable and environmentally friendly materials, play a crucial role in developing active packaging solutions that might enhance the shelf-life of food products. (Li et al., 2022; Mugnaini et al., 2024). In this study, we combined cellulose with tetrabutylammonium hydroxide (TBAH) and zinc salts for the first time as active agents in food packaging. TBAH can be classified within the family of quaternary ammonium compounds (QACs), which can solubilize cellulose and also serve as potent antimicrobial agents for incorporation into food active packaging. (Vilela et al., 2018) QACs consist of a quaternary nitrogen atom bonded to four organic groups, typically alkyl or aryl, with a counter-ion such as chloride or bromide. (Jiao et al., 2017) Their antimicrobial efficacy depends on alkyl chain length, with longer chains generally exhibiting stronger activity. (Arnold et al., 2023; Sola et al., 2023) QACs effectively reduce pathogenic microorganisms responsible for food spoilage, extending shelf life. (Mendoza et al., 2022) However, residues from QAC-based disinfectants can migrate into fat- and protein-rich food matrices if not thoroughly rinsed. (Sidhu et al., 2002) Regulatory limits exist for compounds like benzalkonium chloride and didecyl-dimethyl-ammonium chloride, with maximum residue limits (MRLs) set at 0.1 mg/kg and 0.05 mg/kg, respectively. (Regulation - 396/2005 - EN - EUR-Lex, 2005; Regulation - 2023/377 - EN - EUR-Lex, 2023) The MRL for didecyl-dimethyl-ammonium chloride in plant matrices has been reduced from 0.1 to 0.05 mg/kg. (Regulation - 2023/377 - EN - EUR-Lex, 2023) Unlike these, TBAH lacks specific regulatory limits. TBAH dissolves cellulose by solvating cellulose chains at a 1.2:1 M ratio with glucose monomers, forming fringed micelles—semi-crystalline domains interspersed with amorphous cellulose structures. (Gentile & Olsson, 2016; Gubitosi et al., 2016). The presence of the so-called fringed cellulose micelles have been reported in TBAH.(Gubitosi et al., 2016) Fringed micelles in cellulose refer to structural domains formed within the amorphous and crystalline

* Corresponding author.
E-mail address: luigi.gentile@uniba.it (L. Gentile).

https://doi.org/10.1016/j.foodchem.2025.144494
Received 23 October 2024; Received in revised form 28 March 2025; Accepted 21 April 2025
Available online 22 April 2025
0308-8146/© 2025 The Authors. Published by Elsevier Ltd. This is an open access article under the CC BY license (http://creativecommons.org/licenses/by/4.0/).

regions of cellulose fibers. These micelles are thought to consist of bundles of cellulose chains arranged in semi-crystalline structures. The term "fringed" highlights the partially ordered nature of these regions, where crystalline cores are interspersed with less-ordered, amorphous segments.

Similarly to QACs, zinc salts are widely used in active packaging to enhance food safety and quality. (Li et al., 2022) Zinc plays an essential role in cellular processes across microorganisms and higher organisms, with intracellular Zn^{2+} levels tightly regulated under physiological conditions to prevent toxicity. (Leung et al., 2012; Pasquet et al., 2014; Palmiter & Findley, 1995; Lipovsky et al., 2011) Elevated Zn^{2+} concentrations above optimal levels (typically between 10^{-7} M and 10^{-5} M) (Sugarman, 1983) disrupt zinc homeostasis, leading to Zn^{2+} entry into cells, thereby becoming cytotoxic at concentrations exceeding $\sim 10^{-4}$ M. (Borovanský & Riley, 1989; Sugarman, 1983) Zn^{2+} exhibits antimicrobial properties, and can function as both an antibacterial and antifungal agent. The antimicrobial effects of Zn^{2+} have long been recognized against bacterial (Nagarajan & Rajagopalan, 2008; L. Zhang et al., 2010) and fungal strains.(Miller & McCallan, 1957). These antimicrobial effects are attributed to two mechanisms, both resulting in cell death: (i) direct interaction with microbial membranes causing destabilization and increased permeability; (Mitrić et al., 2010) (ii) interaction with nucleic acids and inhibition of enzymes in the respiratory system. (Fang et al., 2006).

Inorganic salt hydrates represent an alternative to cellulose solvents. (Sen et al., 2013) In comparison to ionic liquids, inorganic salt hydrates offer advantages such as cost-effectiveness, recyclability, low-toxicity, and lower operational temperatures. These salt hydrates penetrate between cellulose fibers, disrupting hydrogen bonds and facilitating cellulose dissolution. (Lara-Serrano et al., 2020; Sen et al., 2013) The structure of salt hydrates is determined by coordination complexation between Cl^- or Br^- anions and water molecules around Zn^{2+} or Li^+ cations. Cellulose is dissolved in hydrate melts only within a narrow hydration window of $3 - x < R < 3 + x$, with $x \approx 1$, with R begging the number of water molecules (Cao et al., 1994; Lu & Shen, 2011; Sen et al., 2016) Moreover, cellulose remains dissolved over the hydrate composition range $3 < R < 9$. (Sen et al., 2016).

Zinc chloride and zinc sulfate play significant roles in cellulose dissolution due to their effectiveness as solvents. Zinc chloride has been extensively investigated for its ability to dissolve cellulose, particularly at high concentrations. Cellulose dissolution in aqueous zinc chloride solutions has been observed at concentrations as high as 63 % (*w*/w) (Jiang et al., 2015) On the other hand, although less studied compared to zinc chloride, zinc sulfate has also demonstrated a potential in dissolving cellulose. (Sen et al., 2013).

In this study, the inclusion of two zinc salts, $ZnCl_2$ and $ZnSO_4$, alongside TBAH, was designed to investigate their combined effects on antifungal activity and the structural properties of cellulose-based colloidal systems. Zinc salts were selected due to their recognized antimicrobial properties and role in enhancing the stability of the cellulose matrix. $ZnCl_2$ and $ZnSO_4$ were specifically chosen to evaluate differences in their interactions with TBAH and cellulose, which could influence their overall efficacy. $ZnCl_2$ is a chloride salt with a smaller ionic radius, while $ZnSO_4$ contains sulfate ions, potentially resulting in varied antifungal mechanisms and effects on the colloidal structure. The use of TBAH as a QAC is, to our knowledge, being reported for the first time in food-related systems.

Here, the combined effect of TBA^+ and Zn^{2+} as antifungal and preservative agents was tested on a relevant fungal phytopathogen affecting cherry tomatoes, placed on food pads impregnated with the active colloidal systems. To prevent the release of TBA^+, which could raise concerns regarding its presence in food intended for human consumption, microcrystalline cellulose was added. The active colloidal systems were characterized by rheology, and the influence of zinc chloride ($ZnCl_2$) and zinc sulfate ($ZnSO_4$) on the dissolution of cellulose in TBAH was highlighted through small-angle X-ray scattering. Finally, ^1H NMR was used to detect any possible traces of TBA^+ in the cherry tomatoes upon storage on the modified food pads.

2. Materials and methods

2.1. Materials

Zinc chloride ($ZnCl_2$), zinc sulfate heptahydrate ($ZnSO_4{\cdot}7H_2O$), and tetrabutylammonium hydroxide (TBAH) 40 wt% in water of chromatographic grade were purchased from Merk Sigma-Aldrich. Avicel PH-101, average particles size of 50 μm, microcrystalline cellulose (MCC) was also acquired from Sigma-Aldrich. All reagents were employed as received. Milli-Q water was used throughout the experiments. Media for fungal growth were purchased from Oxoid (Milan, Italy).

2.2. Sample preparation

The MCC dissolution was obtained following the known procedures in literature (Abe et al., 2012). Essentially, the colloidal systems were prepared by weighing the proper amounts of 40 wt% TBAH and MCC to obtain a 5 wt% of MCC. After the addition of MCC, the solution was vigorously stirred. The dissolution time was approximately 1 h. $ZnCl_2$ and $ZnSO_4{\cdot}7H_2O$ were added progressively to the 5 wt% MCC in 40 wt% TBAH up to a concentration of $8.8{\cdot}10^{-2}$ M. Sample are then labelled as TBAH 5 wt%, TBAH_$ZnCl_2$ 5 wt% and TBAH_$ZnSO_4$ 5 wt%. The 10 mL colloidal systems were prepared for each zinc salt, the "blank" consisting of MCC and TBAH in the absence of salts.

2.3. Food pad activation

The selected pads are commercially available pads (INFIA srl, Bertinoro, FC Italy), used as adsorbent of humidity in plastic boxes used for fruit storage (Fig. 1A). They are mainly made of cellulose, coated with polyethylene. To improve their functionality, the absorbent food pads were infused with cellulose-based colloidal systems containing $ZnCl_2$ and $ZnSO_4$ solutions. Each pad, measuring approximately 12 × 7 cm, was uniformly impregnated with 1.5 mL of the respective solution as described in Section 2.2. The impregnation was achieved manually using a rod-coating system, ensuring a consistent and even distribution of the colloidal system across the entire surface of each pad (Fig. 1B). After coating, the impregnated pads were air-dried at room temperature for 24 h, allowing 90 % water evaporation and stabilizing the colloidal systems within the pad matrix. Three active pads per treatment were placed in plastic containers for *in vivo* tests, while one sterile pad per treatment was cut into 3 × 4 cm pieces for *in vitro* assays.

2.4. In vitro tests of antifungal activity

Portions (3 × 4 cm) of activated pads prepared as reported in paragraph 2.3 were positioned on water agar (20 g agar technical grade in 1 L of distilled water) Petri dishes (6 cm Ø). Unamended pad portions were used as a control. Then, a thin layer made of 3 ml Potato Dextrose Agar was deposited on the pad to serve as a nutrient layer for pathogen growth. Three plates were prepared for each treatment (including the control with unamended pad pieces). Once solid, the plates were inoculated by a 5 mm plug taken from the actively growing margins of 14-day-old colony of *Botrytis cinerea* strain BC28 from the Culture Collection of the Department of Soil, Plant and Food Sciences of the University of Bari Aldo Moro. The plates were incubated for 5 days at 20 ± 1 °C. The area of the pad was considered 100 % infected when completely covered by fungal growth, and 0 % when no growth was observed. Intermediate infection extents were scored accordingly.

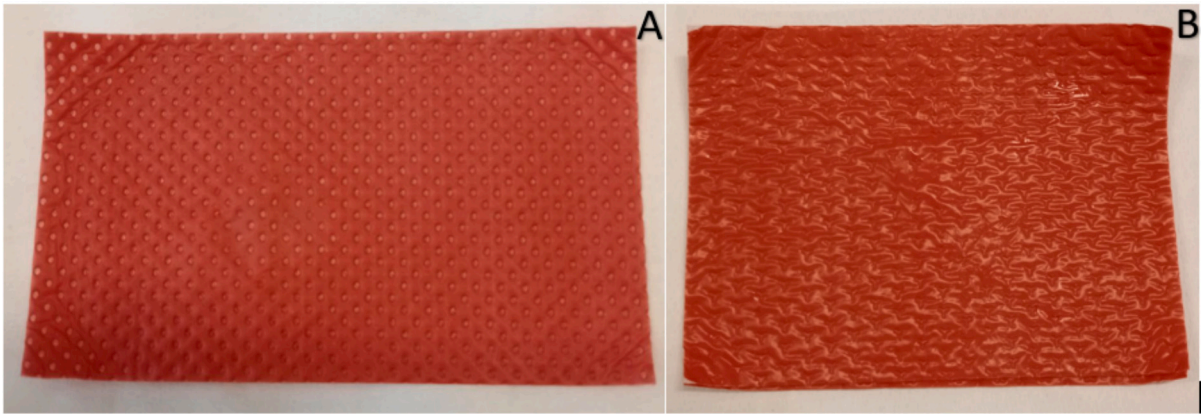

Fig. 1. Food pad (A) and impregnated food pad (B).

2.5. *In vivo tests of activity against fruit rots*

Cherry tomatoes (*Solanum lycopersicon*) of uniform size, colour, and ripeness from organic production were selected. Tomatoes were placed in plastic boxes containing the pads amended with 5 wt% MCC in TBAH (TBAH 5 wt%), aqueous solutions of $ZnCl_2$, or $ZnSO_4$, or the zinc salts solved in presence of MCC in TBAH (TBAH_$ZnCl_2$ 5 wt% and TBAH_$ZnSO_4$ 5 wt%) as reported in paragraph 2.2. Tomatoes in plastic boxes with regular unamended pads were used as a control. For each treatment (and control) 3 replicates of 6 tomatoes each were prepared. The boxes were individually wrapped into polyethylene micro-perforated plastic bags to maintain high relative humidity (80–85 %) and incubated at 20 ± 1 °C for 18 days. They were inspected for the presence of rots at 10, 14 and 18 days of storage (DS) and the percentage of infected fruit (%) calculated as per Eq. 1:

$$\frac{\text{infected fruit n.}}{\text{total fruit n.}} \bullet 100 \tag{1}$$

Data were reported as mean of the replicates ± standard error of the mean (SEM). The experiment was repeated twice.

2.6. *Statistical analysis and synergism evaluation*

For *in vitro* and *in vivo* experiments data were subjected to ANOVA (one-way analysis of variance). Significant differences ($P \leq 0.05$) were identified by the General Linear Model (GLM) procedure with the Duncan's Multiple Range Test (DMRT). The data were processed using the statistical software package Statistics for Windows (StatSoft, Tulsa, OK, USA).

Limpel's formula (Eq. 2), as described by Richer, (Richer, 1987) was used to determine the presence of synergic interactions between compounds in controlling fungal growth and fruit rots.

$$Ee(\%) = (X + Y) - \left(\frac{X \bullet Y}{100}\right) \tag{2}$$

where *Ee* is the expected effect from additive responses of the two controlling compounds used in combination, and *X* and *Y* are the percentages of reduction (CI) of incidence of rots or fungal growth on pads relative to each compound used alone. If the combination of the active agents produced any value of CI greater than *Ee*, synergism exists.

2.7. *Rheology*

Stationary and oscillatory measurements were carried out using a stress-controlled rheometer, Anton Paar MCR302 Anton Paar, Graz, Austria, equipped with a Taylor-Couette geometry (concentric cylinders with inner diameter of 16.662 mm and a 0.704 mm gap). The temperature control was ensured by a Peltier system within ±0.01 °C, using a water bath as Peltier reference.

Stationary experiments were performed in the shear rate, $\dot{\gamma}$, range from 10^{-1} to 10^{3} s^{-1}. The obtained flow curves are modeled with the Carreau-Yasuda model (Gentile et al., 2022) (Eq. 3):

$$\eta = \frac{\eta_{\dot{\gamma}\to 0} - \eta_{\dot{\gamma}\to\infty}}{(1 + (\lambda\dot{\gamma})^{a})^{(1-n)/a}} + \eta_{\dot{\gamma}\to\infty} \tag{3}$$

where η is the apparent viscosity function of the shear rate $\eta(\dot{\gamma})$, $\eta_{\dot{\gamma}\to 0}$ is the zero-shear viscosity, $\eta_{\dot{\gamma}\to\infty}$ is the infinity viscosity, a is a constant that determines the curvature of the transition region (if $a = 2$, Eq. 3 reduces to the Carreau model), n is the flow index, λ is a characteristic time of the system, when $\lambda = 0$, then the fluid becomes Newtonian.

The frequency sweep experiments were performed in the linear viscoelastic regime, *i.e.*, in the small amplitude oscillatory shear (SAOS) conditions using a strain of 10 %. The frequency sweep provided information on the linear viscoelastic behavior in presence and in absence of zinc salts. The complex viscosity (Eq. 4) is given by:

$$|\eta(\omega)^{*}| = \sqrt{(G'/\omega)^{2} + (G''/\omega)^{2}} \tag{4}$$

where G′ is the elastic modulus and G″ is the viscous one, while ω is the angular frequency.

2.8. *Small-angle X-ray scattering (SAXS)*

SAXS experiments were performed with a Xeuss 3.0 (Xenocs, Grenoble, France) working with a 30 W, Cu Kα (1.542 Å) radiation and equipped with a 2D EIGER2R (1 M model) hybrid pixel photon counting detector (Dectris Ltd., Switzerland). Two instrument configurations (sample-to-detector distance 300 and 1700 mm) were used to yield a *q*-range from 0.0094 to 0.6 $Å^{-1}$, where *q* is the magnitude of the scattering vector. Measurements were carried out at around 25 ± 1 °C using glass capillaries (thickness 1.5 mm) as sample holders. Scattering curves were converted in absolute intensity by measuring the scattering from a 1.16 mm thick glassy carbon reference S3 specimen in the same experimental conditions. The scattering measurements were carried out on the MCC in TBAH at 5 wt% in the absence and presence of $ZnCl_2$ and $ZnSO_4{\cdot}7H_2O$. The 1D scattering curves of the samples were obtained by azimuthally averaging the 2D pattern and corrected for TBAH and capillary contributions.

2.9. *Quantitative ^1H nuclear magnetic resonance (^1H NMR)*

The NMR experiments were conducted using an Agilent/Varian VNMRS 500 MHz spectrometer equipped with a OneNMR probe. The ^1H NMR spectra were acquired using the PRESAT pulse sequence for water

suppression. The parameters included 64 number of scans and an acquisition time of 2 s. Cherry tomato samples from experiments in 2.5 were homogenized using a blender before the NMR analysis to ensure accurate and reproducible results. To facilitate the NMR lock, 10 % deuterium oxide (D_2O) was added to the blended tomato juice.

3. Results and discussion

3.1. Rheological characterization of the colloidal systems

The apparent viscosity and the complex viscosity of the colloidal systems prepared by dissolving 5 wt% of MCC in TBAH in the presence of $ZnCl_2$ and $ZnSO_4$ were compared to the colloidal system without salts. The apparent viscosity shows a marginal shear-thinning behavior, almost Newtonian-like, and a similar behavior is seen in the complex viscosity, indicating that no polymeric network is formed, as expected for MCC alone in TBAH. (Gentile & Olsson, 2016; Gubitosi et al., 2016; Brattelli & Gentile, 2025) Interestingly, the presence of $ZnCl_2$ leads to higher viscosities compared to $ZnSO_4$, as shown in Fig. 2. Moreover, the Cox-Merz rule is verified for the system, as can be seen from the inset of Fig. 1B, where $\eta_{\dot{\gamma}\to 0} \cong \eta_{\omega\to 0}$ even in the presence of the salts. Eq. 3 was applied to both apparent viscosity and complex viscosity, and for all systems, $a = 2$, $n = 1$, while the relaxation time λ is approaching zero.

This evidence leads to the hypothesis that cellulose is fully dissolved in TBAH even in the presence of the Zn salts, without forming a polymeric network. This hypothesis is confirmed by the frequency sweep measurements shown in Fig. 3A, even though the systems show a certain shear-thinning behavior.

The frequency sweep measurements reveal a dominant G'' compared to G' across the entire frequency range investigated for all systems, confirming that the cellulose is fully dissolved. Higher G'' favors solution spreading but also implies that, since there is no precipitation, Zn^{2+} is involved in the dissolution process of the cellulose as well as TBAH, lowering ionic mobility. In other words, we can spread the prepared solution onto the food pads, and the cations will be active on their surface, with limited possibility of diffusion onto the tomatoes. Furthermore, the temperature scan reveals the absence of any phase transition even at high temperatures, as the viscosity perfectly follows the Arrhenius law (Fig. 3B).

3.2. Structural characterization of the systems

The shear-thinning character might be due to the presence of fringed micelles made of cellulose chains having a common crystallite unit. How the fringed micelles are affected by the presence of the Zn^{2+} salt can be addressed by SAXS. The 1D SAXS profiles reveal a similar behavior, even though the low-q region is highly affected by the presence of the salts, as seen in Fig. 3. The scattering profiles can be modeled using a second level Beaucage model, (Beaucage, 1996; Hammouda, 2010) (Eq. 5):

$$I(q) = k + \sum_{i=1}^{2}\left[G_i e^{\left(-\frac{q^2R_{gi}^2}{3}\right)} + \frac{B_i\left(erf\left(qR_{gi}/\sqrt{6}\right)\right)^{3pi}}{q^{pi}}\right]. \quad (5)$$

R_{g1} and p_1 are the gyration radius and power slope of the low-q region, respectively; while R_{g2} and p_2 correspond to the high-q region, describing the bump in Fig. 4. G_i and B_i are constants. The R_{gi} and p_i values are reported in Table 1 for all investigated samples.

The R_{g1} and p_1 are highly affected by the presence of salts, indicating a different state of dissolution. In fact R_{g1} is related to the Kuhn length by the Peterlin relationship for the self-avoiding walk (Peterlin, 1953), Eq. 6:

$$\left\langle R_g^2\right\rangle = b^2\frac{N^{2\nu}}{2(1+2\nu)(1+\nu)} \quad (6)$$

In Eq. 6, N is the number of segments equal to $\left(M_z^{MCC}/M_z^g\right)$, where M_z^{MCC} and M_z^g are the z-average molecular weight of the MCC and D-glucose unit, while b is the Kuhn length and ν is the exponent equal to 0.588 in the case of self-avoiding walk.

The Kuhn length is a measure of the stiffness of a polymer chain, and it is closely related to the state of dissolution of a polymer, as it reflects the polymer's effective segment length in a given environment. Changes in solvent quality, temperature, concentration, and the presence of additives can all influence the Kuhn length by altering the polymer's conformation and the interactions between polymer segments and the solvent. Here, for the first time we reported the effect of zinc salts in combination with TBAH on the cellulose dissolution. The estimated Kuhn length increases in presence of Zn^{2+} salts indicating a higher stiffness of the aggregates. Also, the fractal dimension, equal to p_1, increases in the presence of zinc salts. The higher fractal dimension

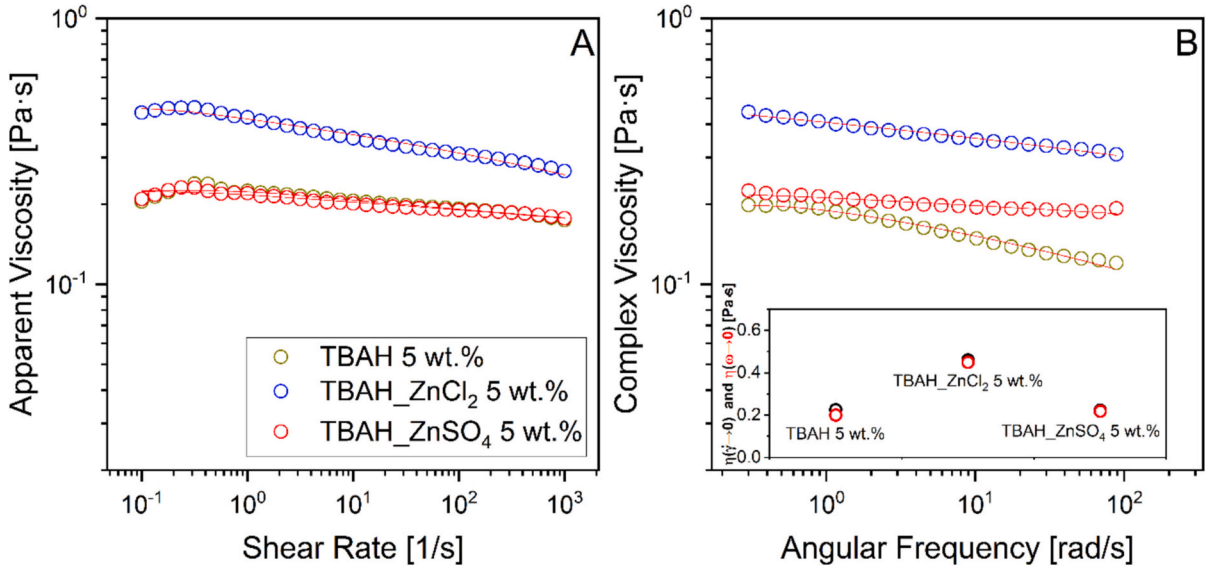

Fig. 2. Apparent (A) and complex viscosity (B) of the 5 wt% MCC in TBAH and of the same colloidal system in the presence of $ZnCl_2$ and $ZnSO_4$ salts. The inset in Fig. 1B represents the zero-shear viscosity and the zero-frequency complex viscosity for the investigated sample. The lines correspond to the Carreau-Yasuda model, Eq. 3.

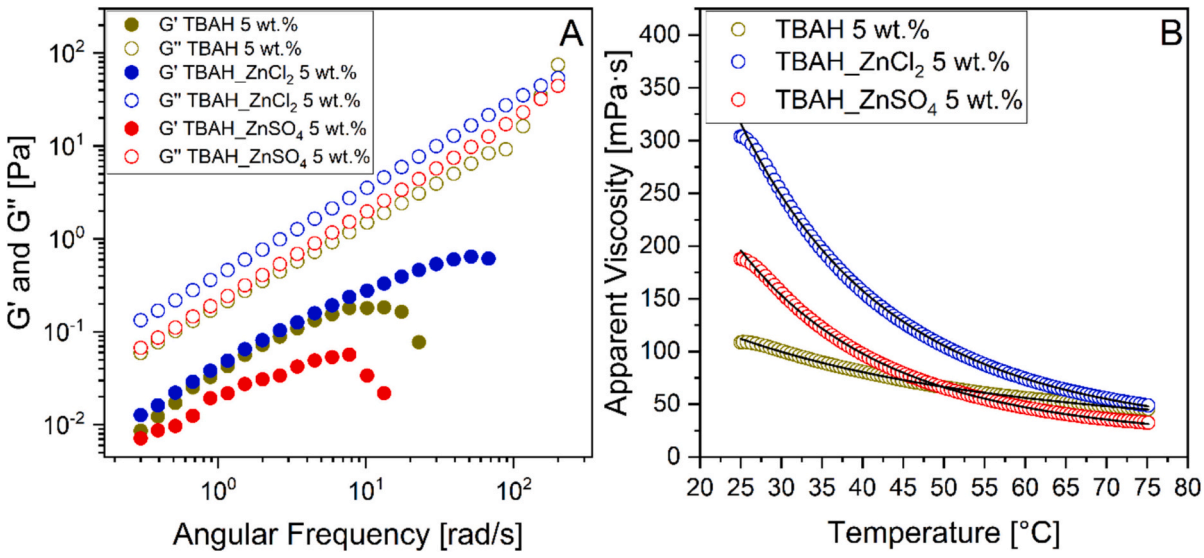

Fig. 3. Frequency sweep measurements (A) and stationary temperature measurements (B) of the 5 wt% MCC in TBAH and the same colloidal system in the presence of $ZnCl_2$ and $ZnSO_4$ salts. The black lines in panel B represent the Arrhenius equation $\eta(T) = Ae^{-E_\eta/RT}$, where A is pre-exponential constant and E_η is the activation energy. The temperature rate was 1 °C/min, and the applied shear rate 1000 s^{-1}.

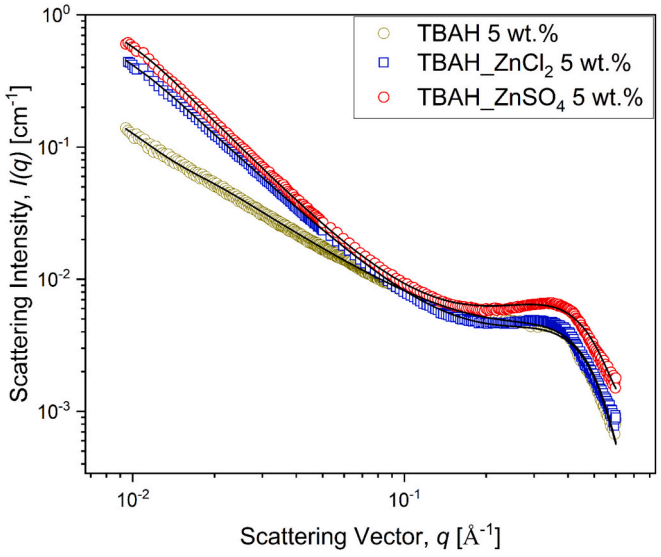

Fig. 4. 1D averaged SAXS profiles of the 5 wt% MCC in TBAH and the same colloidal system in the presence of $ZnCl_2$ and $ZnSO_4$ salts. The black lines represent the fitted Beaucage model, Eq. 5.

Table 1
Radius of gyrations and power law obtained from the Beaucage model, Eq. 5, of the data in Fig. 3, and the Kuhn length *b* obtained applying Eq. 6.

Sample	R_{g1} (nm)*	p_1	b (nm)	R_{g2} (nm)	p_2
TBAH 5 wt%	*21.9*	1.3	2.7	0.45	4
TBAH_$ZnCl_2$ 5 wt%	*38.7*	1.9	4.8	0.45	4
TBAH_$ZnSO_4$ 5 wt%	*38.4*	2.1	4.8	0.45	4

* R_{g1} values are in Italic since the Guinier regime is not reached, even though the values are in agreement with literature. (Gubitosi et al., 2016).

suggests a more compact, dense, and branched structure of the fringed micelles. When the fractal dimension approaches 2, the polymer chains are more tightly packed.

The TBA^+ intercalates between the cellulose fibers, breaking hydrogen bonds and allowing the dissolution of cellulose in a ratio between glucose units and TBA^+ of 1.2. (Gentile & Olsson, 2016) A similar mechanism is reported in literature for salt hydrate. (Awosusi et al., 2017; Hennings et al., 2014; X. Zhang et al., 2018) The structure of salt hydrates is governed by coordination complexation involving Cl^- or SO_4^{2-} anions and H_2O molecules surrounding Zn^{2+} cations. The proposed crystallographic structure of inorganic zinc hydrate for $ZnCl_2$ is {[Zn$(H_2O)_6$][$ZnCl_4$]·$2H_2O$}.(Awosusi et al., 2017; Hennings et al., 2014) It is a complex with an octahedral structure where zinc is surrounded by 6 water molecules $[Zn(H_2O)_6]^{2+}$ and a tetrahedral structure where another zinc is bound to chlorine with additional lattice water molecules. In solution, it has been proposed that the anions of the initial complex {[$Zn(H_2O)_6$][$ZnCl_4$]·$2H_2O$} interact with hydrogen bonds and break them, and the water molecules dissolve the cellulose. (Sen et al., 2016; X. Zhang et al., 2018) A similar explanation could be hypothesized for $ZnSO_4$ leading to {[$Zn(H_2O)_6$][$Zn(SO_4)_2$]·$2H_2O$}.

The presence of both TBA^+ and $[Zn(H_2O)_6]^{2+}$ leads to cellulose dissolution in single chains, and at the same time it increases the fractal dimensions of the fringed micelles, consequently enhancing cellulose aggregates stiffness. In fact, R_{g2} and p_2 are not affected by the presence of salts, since they represent the radius of the polymer chain and the relative Porod exponent, indicating that cellulose is molecularly dissolved even though fringed micelle aggregates are present. At the same time this implies that Zn^{2+}, as well as TBA^+, cations are partially immobilized by the cellulose chains.

3.3. *In vitro* effect of active pads

Rectangular pieces (4 × 3 cm^2) of activated (TBAH_$ZnCl_2$ 5 wt% or TBAH_$ZnSO_4$ 5 wt%) pads (3 × 4 cm) were tested *in vitro* against the fungal pathogen *B. cinerea,* as compared to unamended ones. Pad fragments activated with the individual colloidal systems TBAH 5 wt%, $ZnCl_2$, or $ZnSO_4$ were also included for comparison. Cellulose was excluded, as it was reported to lack specific antifungal properties. (Martini et al., 2014) Data evidenced a complete suppression of fungal growth in presence of TBAH 5 wt% and TBAH_$ZnCl_2$ 5 wt% amended pads (Fig. 5), whereas TBAH_$ZnSO_4$ 5 wt% reduced by 75 % *B. cinerea* growth as compared to the control. The two salts as standalone, at the concentration used to amend the pads, did not impact negatively on fungal growth (Fig. 5). Particularly, in presence of the $ZnCl_2$-amended pads, the fungus grew similarly as compared to the control, whereas in presence of the $ZnSO_4$-amended pads a 40 % increase in fungal growth

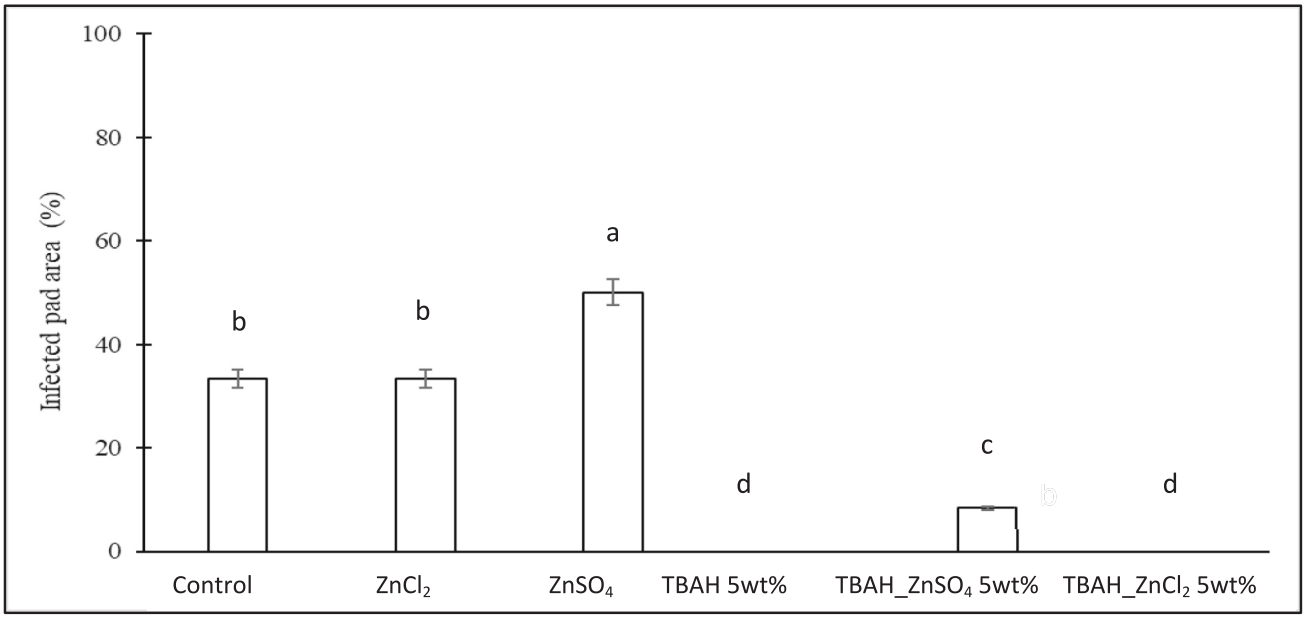

Fig. 5. Infected area (%) of pads untreated (control) or treated with TBAH (TBAH 5 wt%), aqueous solution of $ZnSO_4$ ($ZnSO_4$) or $ZnCl_2$ ($ZnCl_2$), or TBAH containing $ZnCl_2$ (TBAH_$ZnCl_2$ 5 wt%) or $ZnSO_4$ (TBAH_$ZnSO_4$ 5 wt%) in presence of MCC. Pads were embedded in solid medium plates stored at 20 °C for 5 days. Data are the average of three replicates ± standard error of the mean (SEM). Bars with different letter are significantly different ($P \leq 0.05$).

was observed as compared to the control. It is worth noting that zinc salts were in aqueous solution without cellulose, while TBAH_$ZnCl_2$ 5 wt % and TBAH_$ZnSO_4$ 5 wt% were colloidal systems made with 5 wt% of MCC. Thus, despite being partially immobilized by the MCC, the salts seem to benefit from TBAH presence, as their effect in controlling fungal growth as compared to the control was better than when considering them as standalone. The effect of the two compounds in combination proved to be additive according to Limpel's formula. To the best of our knowledge, there are no previous reports of the antifungal activity of TBAH, although its alkaline pH nature might be unfavorable to fungal

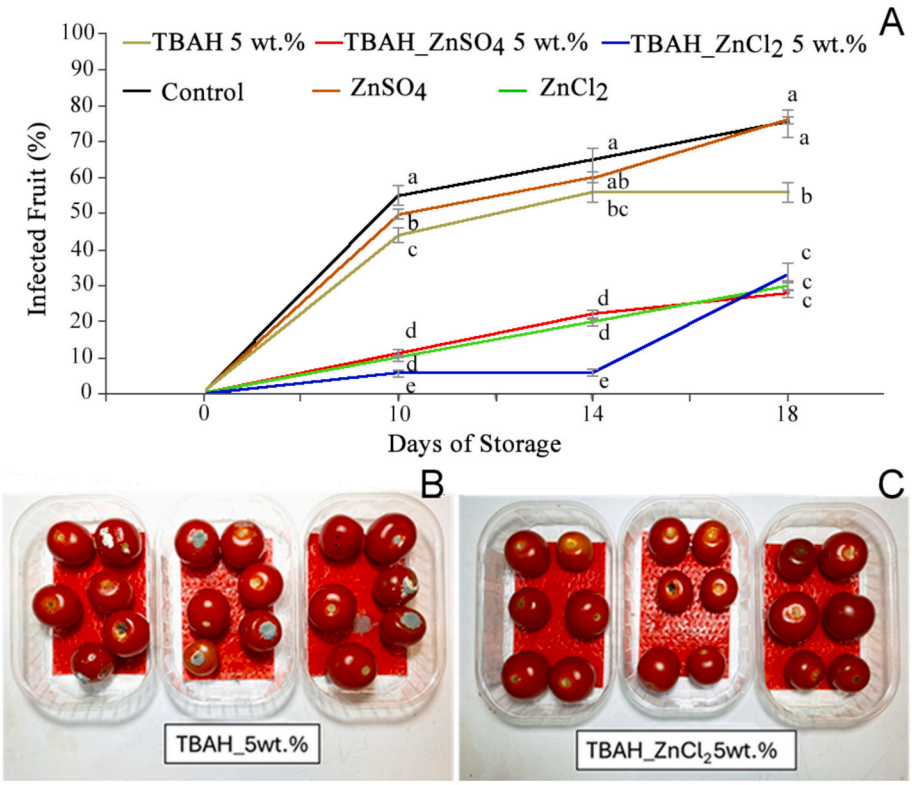

Fig. 6. Infected (%) cherry tomatoes stored at 20 °C for 18 days in plastic boxes containing pads untreated (control), treated with 5 wt% MCC in TBAH (TBAH 5 wt %), aqueous solution of $ZnSO_4$ ($ZnSO_4$) or $ZnCl_2$ ($ZnCl_2$), or TBAH and $ZnCl_2$ (TBAH_$ZnCl_2$ 5 wt%) or $ZnSO_4$ (TBAH_$ZnSO_4$ 5 wt%) in presence of MCC. Data are the average of three replicates ± standard error of the mean (SEM). For each assessment, different letters indicate significant difference ($P \leq 0.05$). (A) Set of cherry tomatoes on food pads treated with TBAH 5 wt% (B) and TBAH_$ZnCl_2$ 5 wt% (C).

growth, as overall fungi prefer acidic pH. (Marianna Sanzani et al., 2021); however, Yu et al. (Yu et al., 2021) reported a robust antibacterial activity by carboxymethyl cellulose derivatives bearing tetrabutylammonium moieties, suggesting the ability of tetraethylammonium moieties addition to carboxymethyl cellulose backbone to improve its antimicrobial activities. Whereas, Zn compounds have been reported to influence growth of several fungi, with a concentration-dependent effect. (Savi et al., 2013).

3.4. *In vivo effect on fruit rots*

Cherry tomatoes stored on activated pads (TBAH_$ZnCl_2$ 5 wt% or TBAH_$ZnSO_4$ 5 wt%) were compared to those stored on unamended ones. Pads containing TBAH 5 wt%, $ZnCl_2$, or $ZnSO_4$ were also included for comparison. $ZnCl_2$ alone showed higher antifungal activity than $ZnSO_4$, probably due to its detrimental effect on chitin synthesis, a key component of the fungal cell wall, as reported in the literature.(Savi et al., 2013) No phytotoxicity phenomena on fruits stored on activated pads were observed. Data (Fig. 6) evidenced that, despite a reduction effect on fruit rot incidence obtained in presence of pads added with TBAH 5 wt% (20 % reduction at 10 DS), $ZnSO_4$ (9 % at 10 DS), or $ZnCl_2$ (82 % at 10 DS), as compared to untreated pads, the combination of zinc salts with TBAH (TBAH_$ZnCl_2$ 5 wt% or TBAH_$ZnSO_4$ 5 wt%) improved the efficacy of active pads. The effect was synergic for TBAH and $ZnSO_4$, and additive for TBAH and $ZnCl_2$. The synergistic effect is most likely due to the conjugation complex formed between $ZnSO_4$ and cellulose, which is mediated by water molecules. Pads with TBAH_$ZnCl_2$ 5 wt% resulted the most effective with a reduction of rots of 89 and 91 % at 10 and 14 DS, respectively, as compared to the control. Pads activated with TBAH_$ZnSO_4$ obtained an 80 and 66 % reduction at 10 and 14 DS, respectively, as compared to the control. This latter treatment had a comparable effect to that obtained in presence of $ZnCl_2$. At 18 DS, TBAH_$ZnCl_2$ 5 wt%, TBAH_$ZnSO_4$ 5 wt%, and $ZnCl_2$ were the best treatments without differences among them. The different effects observed in the *in vivo* assay compared to the *in vitro* assays are not surprising. This discrepancy can be attributed to the presence of host tissues, which may dilute the active principles (particularly in the watery tomato tissues), and the longer contact times between the pathogen and the treated pads, which are possible only in the *in vitro* assays. Furthermore, an induction of host defence responses exerted by active principles might not be excluded. (Martos et al., 2016).

3.5. *TBAH traces in cherry tomatoes*

The tomato juice obtained by blending the tomatoes after their storage on the impregnated food pads was analysed using water-suppressed ^{1}H NMR spectra, to detect possible traces of TBAH. The ^{1}H NMR spectrum of the cherry tomatoes prior to incubation on the impregnated food pads is shown in Fig. 7A, revealing an intense group of resonances in the carbohydrate region from 3 to 4 ppm. In H_2O/D_2O solvents, TBAH resonances appear as a triplet around 0.7–1.0 ppm for the terminal CH_3 protons (labelled as 1 in Fig. 7B), multiplets around 1.2–1.5 ppm for the internal CH_2 protons (2 and 3), and multiplets around 2.8–3.2 ppm for the CH_2 protons adjacent to the nitrogen (4).

To assess the sensitivity of the NMR analysis, the unprocessed cherry tomato juice was intentionally contaminated with 1 and 0.1 mg/kg of TBAH. The signals of TBAH are evident in Fig. 7C for the system having 1 mg/kg TBAH, with slight chemical shift differences due to pH, *i.e.*, from an estimated pH of 14 in Fig. 7B to 4.2 in Fig. 7C. The TBAH signals are not detectable at 0.1 mg/Kg.

The ^{1}H NMR spectra of the cherry tomato juice obtained after 5 and 10 days of storage on the impregnated food pads are presented in Fig. 7D and E. The ^{1}H NMR spectra of tomatoes deposited on the impregnated food pads treated with 5 wt% of MCC in TBAH in the presence of $ZnCl_2$ and $ZnSO_4$ are represented in brown, blue, and red, respectively. No TBAH resonances could be detected in any of the investigated samples,

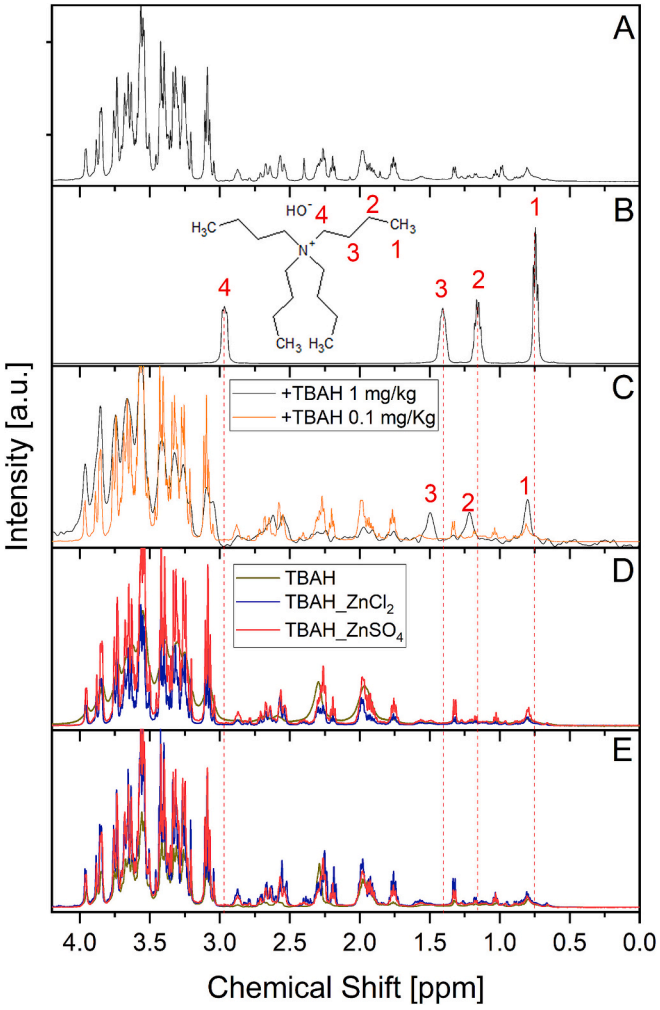

Fig. 7. ^{1}H NMR water-suppressed spectra of (A) fresh cherry tomato juice, (B) TBAH in water, (C) fresh cherry tomato juice with 1 (black) and 0.1 (orange) mg/kg TBAH added, (D) cherry tomato juice obtained from tomatoes left on a modified food pad for 5 days, and (E) cherry tomato juice obtained from tomatoes left on a modified food pad for 10 days. The signal resonances of TBAH are indicated in panel B. Spectra of cherry tomato juice from tomatoes placed on impregnated food pads with 5 wt% of MCC in TBAH, TBAH_$ZnCl_2$, and TBAH_$ZnSO_4$ are shown in brown, blue, and red, respectively. (For interpretation of the references to colour in this figure legend, the reader is referred to the web version of this article.)

suggesting that traces of TBAH, if any, are below or equal to 0.1 mg/kg. (Regulation - 2023/377 - EN - EUR-Lex, 2023; Regulation - 396/2005 - EN - EUR-Lex, 2005).

4. Conclusions

The modification of absorbent food pads with cellulose-based active colloidal systems, incorporating inorganic salts and TBAH, has demonstrated promising results in extending the shelf life of cherry tomatoes. The *in vitro* tests showed a complete suppression of fungal growth by TBAH alone and the combination of TBAH with $ZnCl_2$ in presence of 5 wt % cellulose. While neither TBAH nor the zinc salts alone affected fungal growth at the concentrations used, the combination of these compounds in a cellulose-based colloidal system proved effective, with a synergistic interaction between TBAH and $ZnSO_4$ and an additive effect for TBAH and $ZnCl_2$. The proposed mechanism suggests that the presence of zinc alters the fractal dimension and stiffness of the cellulose fringed micelles without affecting their overall rheological response. The presence of

MCC did not alter the efficiency of the active compound, despite structural and rheological characterization of the colloidal systems confirming the absence of a polymeric network. However, MCC partially immobilizes Zn^{2+} and TBA^{+} cations, restricting their diffusion into other aqueous matrices, while being available on the substrate surface to interact molecularly with the microbial membrane.

In vivo results further supported the antifungal efficacy of the active pads: samples treated with 5 wt% MCC in TBAH in the presence of $ZnCl_2$ reduced fruit rot by 89 % and 91 % at 10 and 14 days of storage, respectively, compared to the control. Pads treated with 5 wt% MCC in TBAH in the presence of $ZnSO_4$ achieved 80 % and 66 % reduction over the same period. Pads with 5 wt% MCC in TBAH in the presence of $ZnCl_2$ remained the most effective throughout the entire storage period, with significant reductions in fungal rots up to 18 days. This suggests that combining TBAH with zinc salts offers an enhanced approach for controlling fungal-induced spoilage in horticultural products.

Moreover, no significant TBAH contamination of the cherry tomatoes was detected by ^{1}H NMR in all investigated samples, confirming that TBAH concentration is below the limit reported to be acceptable for human health, in case of similar quaternary ammonium species. The low TBA^{+} release is due to its partial immobilization by the cellulose chains, which limits its diffusion into other aqueous matrices. These findings underscore the potential of cellulose-based active colloidal dispersions for antimicrobial food pads, though further research is warranted to optimize formulation and minimize long-term exposure potential risks. To enhance the practical applicability of the proposed system, further consideration of its scalability and cost-effectiveness is needed, especially given the high cost of TBAH. Future studies will focus on the use of TBAH in food-related systems, while also exploring greener alternatives. Additionally, potential limitations, such as the environmental impacts of TBAH use and the need for long-term studies to further validate the findings, will be addressed.

CRediT authorship contribution statement

Andrea Brattelli: Investigation, Data curation. **Maria Chiara Sportelli:** Writing – review & editing, Project administration, Methodology, Funding acquisition, Data curation. **Rosaria Anna Picca:** Methodology. **Nicola Cioffi:** Writing – review & editing, Project administration, Methodology, Funding acquisition. **Mara Pasqualicchio:** Writing – review & editing, Methodology. **Ornella Incerti:** Writing – review & editing. **Simona Marianna Sanzani:** Writing – original draft, Project administration, Methodology, Investigation, Funding acquisition, Data curation. **Luigi Gentile:** Writing – review & editing, Writing – original draft, Supervision, Project administration, Methodology, Investigation, Funding acquisition, Data curation, Conceptualization.

Declaration of competing interest

The authors declare that they have no known competing financial interests or personal relationships that could have appeared to influence the work reported in this paper.

Acknowledgments

All authors acknowledge the Italian Project IAO “Imballaggio Attivo Ortofrutticoli”, Grant n° J98H23000070008, from the “Ministero dell’Agricoltura, della Sovranità Alimentare e delle Foreste”. L.G. was funded by Italian Ministry of University and Research (MUR) under the program Italian Science Fund (FIS 2021), Starting Grant number [FIS00003259]. O.I. acknowledges the project “ON Foods - Research and innovation network on food and nutrition Sustainability, Safety and Security – Working ON Foods”, code PE00000003, by the Italian Ministry of University and Research (MUR), CUP D93C22000890001, funded under the National Recovery and Resilience Plan (NRRP), Mission 4 Component 2 Investment 1.3 - Call for tender No. 341 of 15 March 2022 of MUR funded by the European Union – NextGenerationEU.

Data availability

Data will be made available on request.

References

Abe, M., Fukaya, Y., & Ohno, H. (2012). Fast and facile dissolution of cellulose with tetrabutylphosphonium hydroxide containing 40 wt% water. *Chemical Communications, 48*(12), 1808–1810. https://doi.org/10.1039/c2cc16203b

Ahmed, M. W., Haque, M. A., Mohibbullah, M., Khan, M. S. I., Islam, M. A., Mondal, M. H. T., & Ahmmed, R. (2022). A review on active packaging for quality and safety of foods: Current trends, applications, prospects and challenges. *Food Packaging and Shelf Life, 33*. https://doi.org/10.1016/j.fpsl.2022.100913

Arnold, W. A., Blum, A., Branyan, J., Bruton, T. A., Carignan, C. C., Cortopassi, G., … Zheng, G. (2023). Quaternary ammonium compounds: A chemical class of emerging concern. *Environmental Science and Technology, 57*(20), 7645–7665. https://doi.org/10.1021/acs.est.2c08244

Awosusi, A. A., Ayeni, A., Adeleke, R., & Daramola, M. O. (2017). Effect of water of crystallization on the dissolution efficiency of molten zinc chloride hydrate salts during the pre-treatment of corncob biomass. *Journal of Chemical Technology and Biotechnology, 92*(9), 2468–2476. https://doi.org/10.1002/jctb.5266

Beaucage, G. (1996). Small-angle scattering from polymeric mass fractals of arbitrary mass-fractal dimension. *Journal of Applied Crystallography, 29*(2), 134–146. https://doi.org/10.1107/S0021889895011605

Borovanský, J., & Riley, P. A. (1989). Cytotoxicity of zinc in vitro. *Chemico-Biological Interactions, 69*(2–3), 279–291. https://doi.org/10.1016/0009-2797(89)90085-9

Brattelli, A., & Gentile, L. (2025). Adsorbent semi-transparent cellulose-based self-standing thin films. *Carbohydrate Polymers, 359*, 123584. https://doi.org/10.1016/j.carbpol.2025.123584

Cao, N. J., Xu, Q., Chen, C. S., Gong, C. S., & Chen, L. F. (1994). Cellulose hydrolysis using zinc chloride as a solvent and catalyst. *Applied Biochemistry and Biotechnology, 45–46*(1), 521–530. https://doi.org/10.1007/BF02941827

Fang, M., Chen, J. H., Xu, X. L., Yang, P. H., & Hildebrand, H. F. (2006). Antibacterial activities of inorganic agents on six bacteria associated with oral infections by two susceptibility tests. *International Journal of Antimicrobial Agents, 27*(6), 513–517. https://doi.org/10.1016/j.ijantimicag.2006.01.008

Gentile, L., & Olsson, U. (2016). Cellulose–solvent interactions from self-diffusion NMR. *Cellulose, 23*(4). https://doi.org/10.1007/s10570-016-0984-0

Gentile, L., Sixta, H., Giannini, C., & Olsson, U. (2022). A novel X-ray diffraction approach to assess the crystallinity of regenerated cellulose fibers. *IUCrJ, 9*, 492–496. https://doi.org/10.1107/S205225252200570X

Gubitosi, M., Duarte, H., Gentile, L., Olsson, U., & Medronho, B. (2016). On cellulose dissolution and aggregation in aqueous tetrabutylammonium hydroxide. *Biomacromolecules, 17*(9). https://doi.org/10.1021/acs.biomac.6b00696

Hammouda, B. (2010). Analysis of the Beaucage model. *Journal of Applied Crystallography, 43*(6), 1474–1478. https://doi.org/10.1107/S0021889810033856

He, M., Pan, J., Hong, M., Shen, Y., Zhang, H., Jiang, Y., & Gong, L. (2024). Fabrication of antimicrobial packaging based on polyaminopropyl biguanide incorporated pectin/polyvinyl alcohol films for fruit preservation. *Food Chemistry, 457*, Article 140106. https://doi.org/10.1016/J.FOODCHEM.2024.140106

Hennings, E., Schmidt, H., & Voigt, W. (2014). Crystal structures of ZnCl2·2.5H2O, ZnCl2·3H2O and ZnCl2·4.5H2O. *Acta Crystallographica section E: Structure reports Online, 70*(12), 515–518. https://doi.org/10.1107/S1600536814024738

Jiang, X., Han, J., Han, Q., Zhou, X., & Ma, J. (2015). Preparation and characteristics of paper-based biodegradable plastics. *BioResources, 10*(2), 2982–2994. https://doi.org/10.15376/biores.10.2.2982-2994

Jiao, Y., Niu, Na, L., Ma, S., Li, J., Tay, F. R., & Chen, J. H. (2017). Quaternary ammonium-based biomedical materials: State-of-the-art, toxicological aspects and antimicrobial resistance. *Progress in Polymer Science, 71*, 53–90. https://doi.org/10.1016/j.progpolymsci.2017.03.001

Kadirvel, V., Palanisamy, Y., & Ganesan, N. D. (2025). Active packaging system—An overview of recent advances for enhanced food quality and safety. *Packaging Technology and Science, 38*(2), 145–162. https://doi.org/10.1002/PTS.2863

Kumari, S., Debbarma, R., Nasrin, N., Khan, T., Taj, S., & Bhuyan, T. (2024). Recent advances in packaging materials for food products. *Food Bioengineering, 3*(2), 236–249. https://doi.org/10.1002/FBE2.12096

Lara-Serrano, M., Fierro, J. L. G., Morales-Delarosa, S., & Campos-Martín, J. M. (2020). High enhancement of the hydrolysis rate of cellulose after pretreatment with inorganic salt hydrates. *Green Chemistry, 22*(12), 3860–3866. https://doi.org/10.1039/d0gc01066a

Leung, Y. H., Chan, C. M. N., Ng, A. M. C., Chan, H. T., Chiang, M. W. L., Djurišić, A. B., … Au, D. T. W. (2012). Antibacterial activity of ZnO nanoparticles with a modified surface under ambient illumination. *Nanotechnology, 23*(47). https://doi.org/10.1088/0957-4484/23/47/475703

Li, X., Zhang, R., Hassan, M. M., Cheng, Z., Mills, J., Hou, C., … Hicks, T. M. (2022). Active packaging for the extended shelf-life of meat: Perspectives from consumption habits, Market Requirements and Packaging Practices in China and New Zealand. *Foods, 11*(18). https://doi.org/10.3390/foods11182903

Lu, X., & Shen, X. (2011). Solubility of bacteria cellulose in zinc chloride aqueous solutions. *Carbohydrate Polymers, 86*(1), 239–244. https://doi.org/10.1016/j.carbpol.2011.04.042

Marianna Sanzani, S., Sgaramella, M., Mosca, S., Solfrizzo, M., Ippolito, A., Editors, A., Di Francesco, A., Romanazzi, G., Torres, R., & Merah, O. (2021). Control of Penicillium expansum by an epiphytic Basidiomycetous yeast. *Horticulturae, 7*(11), 473. https://doi.org/10.3390/HORTICULTURAE7110473

Martini, R., Serrano, L., Barbosa, S., & Labidi, J. (2014). Antifungal cellulose by capsaicin grafting. *Cellulose, 21*(3), 1909–1919. https://doi.org/10.1007/S10570-014-0219-1/METRICS

Martos, S., Gallego, B., Cabot, C., Llugany, M., Barceló, J., & Poschenrieder, C. (2016). Zinc triggers signaling mechanisms and defense responses promoting resistance to Alternaria brassicicola in Arabidopsis thaliana. *Plant Science, 249*, 13–24. https://doi.org/10.1016/J.PLANTSCI.2016.05.001

Mendoza, I. C., Luna, E. O., Pozo, M. D., Vásquez, M. V., Montoya, D. C., Moran, G. C., … León, J. C. (2022). Conventional and non-conventional disinfection methods to prevent microbial contamination in minimally processed fruits and vegetables. *Lwt, 165*. https://doi.org/10.1016/j.lwt.2022.113714

Miller, L. R., & McCallan, S. E. A. (1957). Fungicides, toxic action of metal ions to fungus spores. *Journal of Agricultural and Food Chemistry, 5*(2), 116–122. https://doi.org/10.1021/jf60072a003

Mitrić, M., Stanić, V., Jokić, B., Plećaš, I. B., Antić-Stanković, J., Raičević, S., & Dimitrijević, S. (2010). Synthesis, characterization and antimicrobial activity of copper and zinc-doped hydroxyapatite nanopowders. *Applied Surface Science, 256*(20), 6083–6089.

Mugnaini, G., Bonini, M., Gentile, L., Panza, O., Del Nobile, M. A., Conte, A., … Panzella, L. (2024). Effect of design and molecular interactions on the food preserving properties of alginate/pullulan edible films loaded with grape pomace extract. *Journal of Food Engineering, 361*. https://doi.org/10.1016/j.jfoodeng.2023.111716

Nagarajan, P., & Rajagopalan, V. (2008). Enhanced bioactivity of ZnO nanoparticles—An antimicrobial study. *Science and Technology of Advanced Materials, 9*(3), 35004. http://stacks.iop.org/1468-6996/9/i=3/a=035004.

Pasquet, J., Chevalier, Y., Pelletier, J., Couval, E., Bouvier, D., & Bolzinger, M. A. (2014). The contribution of zinc ions to the antimicrobial activity of zinc oxide. *Colloids and Surfaces A: Physicochemical and Engineering Aspects, 457*(1), 263–274. https://doi.org/10.1016/j.colsurfa.2014.05.057

Peterlin, A. (1953). Modèle statistique des grosses molécules à chaînes courtes. V. Diffusion de la lumière. *Journal of Polymer Science, 10*(4), 425–436. https://doi.org/10.1002/pol.1953.120100405

Regulation - 2023/377 - EN - EUR-Lex. (2023). https://eur-lex.europa.eu/eli/reg/2023/377/oj.

Regulation - 396/2005 - EN - EUR-Lex. (2005). L 70 Official Journal of the European Union 1. http://data.europa.eu/eli/reg/2005/396/oj.

Richer, D. L. (1987). Synergism—A patent view. *Pesticide Science, 19*(4), 309–315. https://doi.org/10.1002/PS.2780190408

Savi, G. D., Bortoluzzi, A. J., & Scussel, V. M. (2013). Antifungal properties of zinc-compounds against toxigenic fungi and mycotoxin. *International Journal of Food Science & Technology, 48*(9), 1834–1840. https://doi.org/10.1111/IJFS.12158

Sen, S., Losey, B. P., Gordon, E. E., Argyropoulos, D. S., & Martin, J. D. (2016). Ionic liquid character of zinc chloride hydrates define solvent characteristics that afford the solubility of cellulose. *Journal of Physical Chemistry B, 120*(6), 1134–1141. https://doi.org/10.1021/acs.jpcb.5b11400

Sen, S., Martin, J. D., & Argyropoulos, D. S. (2013). Review of cellulose non-derivatizing solvent interactions with emphasis on activity in inorganic molten salt hydrates. *ACS Sustainable Chemistry and Engineering, 1*(8), 858–870. https://doi.org/10.1021/SC400085A/ASSET/IMAGES/MEDIUM/SC-2013-00085A_0007.GIF

Sidhu, M. S., Sørum, H., & Holck, A. (2002). Resistance to quaternary ammonium compounds in food-related bacteria. *Microbial Drug Resistance, 8*(4), 393–399. https://doi.org/10.1089/10766290260469679

Sola, E. A., Bourilhón, P., Manzo, R. M., & Frisón, L. N. (2023). Antifungal action of quaternary ammonium compounds against environmental molds isolated from food industries. *Journal of Food Safety, 43*(1), Article e13017. https://doi.org/10.1111/JFS.13017

Stroescu, M., Isopencu, G., Busuioc, C., & Stoica-Guzun, A. (2019). *Antimicrobial food pads containing bacterial cellulose and polysaccharides*, 1303–1338. https://doi.org/10.1007/978-3-319-77830-3_3

Su, J., Zhang, W., Moradi, Z., Rouhi, M., Parandi, E., & Garavand, F. (2025). Recent functionality developments of carboxymethyl chitosan as an active food packaging film material. *Food Chemistry, 463*, Article 141356. https://doi.org/10.1016/J.FOODCHEM.2024.141356

Sugarman, B. (1983). Zinc and infection. *Reviews of Infectious Diseases, 5*(1), 137–147. https://doi.org/10.1093/clinids/5.1.137

Vilela, C., Kurek, M., Hayouka, Z., Röcker, B., Yildirim, S., Antunes, M. D. C., … Freire, C. S. R. (2018). A concise guide to active agents for active food packaging. *Trends in Food Science and Technology, 80*, 212–222. https://doi.org/10.1016/j.tifs.2018.08.006

Xu, M., Liu, S., Wen, J., Wang, B., Wang, H., Lian, X., Gao, X., Niu, B., & Li, W. (2024). Preparation of sodium alginate modified silver-metal organic framework and application in citric acid/PVA antimicrobial packaging. *Food Chemistry, 451*, Article 139464. https://doi.org/10.1016/J.FOODCHEM.2024.139464

Yu, J., Wang, L., Zhao, Y., & Zhou, C. (2021). Preparation, characterization, and antibacterial property of carboxymethyl cellulose derivatives bearing tetrabutylammonium salt. *International Journal of Biological Macromolecules, 176*, 72–77. https://doi.org/10.1016/J.IJBIOMAC.2021.02.063

Zhang, L., Jiang, Y., Ding, Y., Daskalakis, N., Jeuken, L., Povey, M., … York, D. W. (2010). Mechanistic investigation into antibacterial behaviour of suspensions of ZnO nanoparticles against E. Coli. *Journal of Nanoparticle Research, 12*(5), 1625–1636. https://doi.org/10.1007/s11051-009-9711-1

Zhang, X., Xiao, N., Wang, H., Liu, C., & Pan, X. (2018). Preparation and characterization of regenerated cellulose film from a solution in lithium bromide molten salt hydrate. *Polymers, 8*(6). https://doi.org/10.3390/polym10060614